Available online at www.sciencedirect.com

jmr&t Journal of Materials Research and Technology

journal homepage: www.elsevier.com/locate/jmrt

Behavior of stiffened concrete-filled steel tube columns infilled with nanomaterial-based concrete subjected to axial compression

Harpreet Singh [a], *Aditya Kumar Tiwary* [a,b], *Sayed M. Eldin* [c,*], *R.A. Ilyas* [d,e,f,g,**]

[a] *Department of Civil Engineering, University Institute of Engineering, Chandigarh University, Mohali, 140413, Punjab, India*

[b] *University Center for Research and Development, Chandigarh University, Mohali, 140413, Punjab, India*

[c] *Centre of Research, Faculty of Engineering, Future University in Egypt, New Cairo, 11835, Egypt*

[d] *Department of Chemical Engineering, Faculty of Chemical and Energy Engineering, Universiti Teknologi Malaysia, 81310, UTM Johor Bahru, Johor, Malaysia*

[e] *Centre for Advanced Composite Materials, Universiti Teknologi Malaysia, 81310, UTM Johor Bahru, Johor, Malaysia*

[f] *Institute of Tropical Forestry and Forest Products, Universiti Putra Malaysia, Serdang, 43400, Selangor, Malaysia*

[g] *Centre of Excellence for Biomass Utilization, Universiti Malaysia Perlis, 02600, Arau, Perlis, Malaysia*

ARTICLE INFO

Article history:
Received 24 February 2023
Accepted 15 May 2023
Available online 18 May 2023

Keywords:
Thin-walled concrete-filled double skin steel tube section
Catty-cornered propped CFST
Stiffened CFST
Ultimate load capacity
Load-strain behavior
Composite action

ABSTRACT

The use of nanotechnology in the field of construction emerged as the utilization of nanomaterials to improve the mechanical properties of concrete. In this study, a novel form of stiffening scheme was suggested, named a catty-cornered propped concrete-filled steel tube (CFST) column. The performance of the suggested stiffened CFST column was analyzed under axial compression. The steel tube of CFST specimens was filled with normal and nanomaterial-based concrete. The three kinds of nanomaterials were utilized viz., nano-silica (NS), carbon nanotubes (CNT), and nano-titanium dioxide (NT). The results of the investigation were collected in terms of ultimate capacity, load vs strain behavior, and load vs deformation response. The ductility index (DI), secant stiffness, composite interaction, and confining effect variation were also discussed further. It was observed that the suggested stiffening scheme was able to increase the ultimate capacity of unstiffened CFST by approximately 14%. The use of nanomaterials in CFST infill concrete also resulted in an approximately 7% increase in load capacity. Further increasing the number of stiffening bars improved the ductility and stiffness of the column section. On the other hand, the inclusion of nanomaterials resulted in a decrease in the ductility index and improved the stiffness of the section. The proposed stiffening scheme resulted in better composite interaction and increased confinement. It was also concluded that the utilization of nanomaterial-based concrete as an infill in the stiffened CFST column could enhance its performance under axial compression loading.

* Corresponding author.
** Corresponding author.
E-mail addresses: sayed.eldin22@fue.edu.eg (S.M. Eldin), ahmadilyas@utm.my (R.A. Ilyas).

https://doi.org/10.1016/j.jmrt.2023.05.135

1. Introduction

About 40% of the energy used in economic growth is utilized by the construction industry [1–3]. Concrete is widely utilized in the construction market because of its economical price and strong mechanical qualities. Cement is the main element of concrete that increases the carbon footprint. The CO_2 emissions from cement production make up roughly 5% of the overall global carbon dioxide emissions [4,5]. In order to increase concrete's sustainability, efficacy, and durability over the course of its safety service life, a number of additional cementitious elements have been added [6–8]. Although there are many benefits to employing these materials, there are drawbacks as well since, when utilized on a big scale, their delayed setting time and early age strength present problems. Meanwhile, Because of their distinctive characteristics and extremely small particle sizes, nanoparticles have drawn significant attention and are used in a wide range of engineering projects. Concrete has been modified with various kinds of nanoparticles to augment its mechanical and durability characteristics [9–11]. The experiments were conducted in past to evaluate the effect of carbon nanotube (CNT)-rice husk (RHA) ash and multiwalled carbon nanotubes (MWCNT)-recycled concrete aggregate (RCA) combinations in the concrete. It was deduced that concrete mixed with rice husk ash gave better sustainability outcomes. The addition of 5% of rice husk ash in replacement for cement led to a reduction in carbon emission and energy consumption in the cement production process. It was noted that slump values were reduced due to the addition of MWCNT, however, impact resistance and compressive strength of RCA were increased with the use of MWCNT [12,13]. The studies were also conducted on concrete designed with titanium dioxide (TiO_2) as a nanoparticle and rice husk ash (RHA) as the cementitious substance for partially replacing concrete. The strength and durability of concrete were highly improved when 10% RHA and 3% TiO_2 were employed. It was concluded that 3% of TiO_2 replacement might be taken as the optimum amount [14]. Additionally, micro- and nano-silica (MS and NS) particles have demonstrated a significant gain in utilization in the concrete mix. With a significant improvement in their mechanical properties, particularly compressive strength, concrete seems to have become denser [15]. The combined usage of nano-silica, silica fume, and steel slag with normal concrete minorly enhanced the strength property, however, up to a certain limit, beyond which strength was reduced [16].

Concrete-filled steel tubular (CFST) members are frequently employed in the construction sector, and the application of light gauge steel tubular sections has grown in the last few decades for applications in engineering structures [17]. The features of both hollow structural steel and the concrete core are implemented in concrete-filled steel tube (CFST)-based composite structures [18–20]. CFST members maintain strong resistance to vibrations caused by static and earthquakes because of their high strength, high ductility, and enormous energy absorption capacity [21]. Infilled concrete is an essential component in CFST columns; the CFST members with different infills viz., normal concrete, ultra-high strength concrete, self-compacting concrete, and concrete with crumb rubber, etc. Were tested and imposed to uniaxial compressive forces. Lightweight concrete infill CFST was found to be had better confinement effect as compared with ultrahigh strength concrete infill [22,23]. The CFST columns with nano silica-based concrete as infill material seemed to provide higher bearing strength and improvement in the ductile ability. The localized buckling resistance was 4% more in the case of nano silica-based infill CFST as compared with normal concrete infill CFST [24]. Also, the impact of self-compacting concrete as infill material in CFST to upgrade the bonding in CFST columns was assessed. It was observed the self-compacting concrete with steel slag aggregates reflect the enhancement in bond strength for both square and circular shape columns [25]. The CFST column, however, may be subject to local buckling, which caused a decrease in the load-carrying capacity. Various measure was adopted in past to stiffen the CFST section and to eliminate such localized failures.

Numerous studies explored how binding bar-type stiffeners performed [26,27]. Binding bars seemed to boost the exterior steel casing's constraining force on the concrete and postpone localized buckling [28]. Saw-shaped stiffeners [29] were utilized in concrete infill together with binding bars and steel fibers to increase the ductile ability. According to observations, incorporating steel fiber into concrete was the most effective way to augment the ductile nature of CFST specimens. The behavior of other stiffeners, such as tensile bars which were circular, triangular, battlement-shaped, and inclined battlement-shaped either with or without longitudinal ribs and rods, was also studied by several other researchers [30,31]. The maximum load-bearing ability and ductility of tensile bars with ring and inclined battlement shapes were better, but fabrication was more challenging. Yang et al. [32] revealed that ring bars and orthogonal tensile rods significantly outperformed tensile rods with an indented battlement shape. In addition, Ding et al. [33] observed that despite having little effect on ultimate strength, the use of headed studs boosted the section's ductility. Tao et al. [29,34] examined the efficacy of both square and rectangular CFST sections in the influence of plate stiffeners with vertical ribs. It was revealed that the outer steel casing's axial load-bearing ability and local buckling resistance had improved. A particular kind of stiffener designated as PBL (Perfobond Leister), which comprises plate stiffeners having holes drilled in them, was used by many authors [35–37]. PBL stiffeners were demonstrated to impact steel tube deformation, but they had little to no effect on ultimate bearing strength. Inclined plates were proposed by Liang et al. as an innovative type of stiffener. In order to avoid local tube buckling, boost ultimate strength, and optimize ductility, these stiffening arrangements worked effectively. Furthermore, improvements of this kind applied to all four sides of the tube outperform those applied to only two sides [38]. The performance of a square CFST with a group of four diagonal bars or inclined tie rods at the corners was explored by Huang et al. [39] and Hu et al. [40]. This type of stiffener boosts the CFST section's buckling resistance, ultimate strength, and ductile ability. To further improve the interface between the steel tube and the filler material (concrete) U-shaped tension bars were recommended by Wang et al. [41], and findings revealed that these

alterations improved buckling resistance and made the section more ductile.

In essence, stiffeners, when employed with conventional CFST columns, increase the ultimate load-bearing capacity. Some stiffeners, although, do not improve ductility; rather, they prevent local steel tube buckling. The current study presents a novel stiffening configuration due to difficulties in providing well-known varieties of stiffeners. The suggested arrangement consists of an outer steel casing with steel reinforcing bars positioned internally and diagonally from one end to the other, followed by concrete filling. The column is termed a "Catty-Cornered Propped CFST" column. A circular cross-section is employed for columns due to its greater post-yield strength and stiffness than a square cross-section and is more effective at providing confining effect [42]. Additionally, there is a scarcity of research on how CFST behaves with various types of infill materials since the strength of CFST is strongly dependent on the infill material (often concrete). The current study included an experimental evaluation of suggested CFST specimens subjected to uniaxial compressive loading with infill concrete supplemented with nanomaterials. The performance of proposed catty-cornered propped CFST columns with nanomaterial-based concrete was assessed through ultimate load capacity, load vs strain behavior, and load vs deformation curves. Further, the ductile behavior, stiffness, confining pressure, and composite interaction between steel casing and concrete infill were explored at the end.

2. Experimental program

2.1. Test specimen

The experiments were performed to assess the suggested catty-cornered propped CFST columns with infill concrete properties enhanced with the use of nanomaterials. The typical layout of the suggested CFST is presented in Fig. 1. The steel casing with an outer size of 180 mm and a tube thickness of 3 mm was considered. All the specimen was of the same length as 540 mm, with length to diameter ratio of 3, and were considered stub columns. The catty-cornered props were provided from the top end to the bottom end diagonally. The diameter of the prop bar was considered as 12 mm and different configurations of props were used such as binary props, tertiary props, and quaternary props, and their details are shown in Figs. 2 and 3. The specimens were made as unstiffened CFST specimens and stiffened CFST specimens with binary props, tertiary props, and quaternary props. The nanomaterials were utilized in infill concrete to enhance its properties. Accordingly, a greater number of specimens were cast using nano-silica, carbon nanotubes, and nano-titanium dioxide-modified concrete. The details of the specimens were shown in Table 1. In Table 1, specimen abbreviation is as follows: UC stands for unstiffened CFST, BSC stands for binary propped stiffened CFST, TSC implies tertiary propped stiffened CFST, QSC implies quaternary propped stiffened CFST,

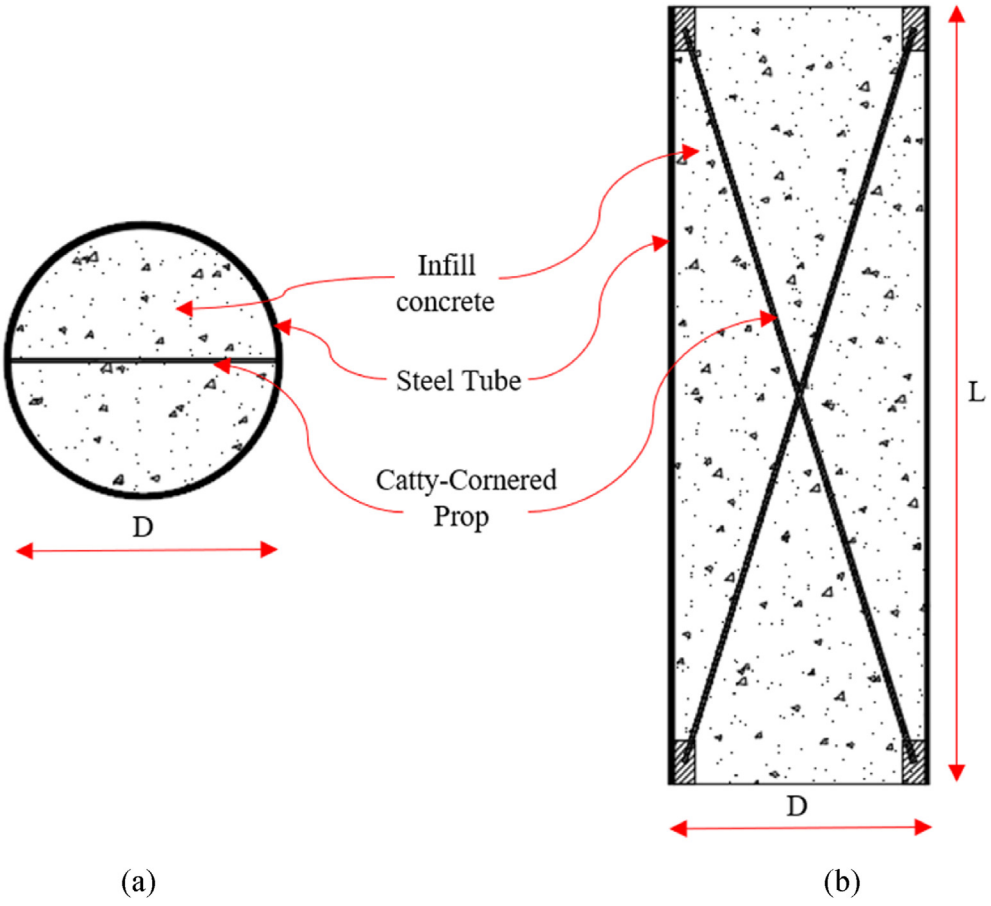

Fig. 1 – Layout of catty-cornered propped CFST, (a) Top view, (b) Elevation view.

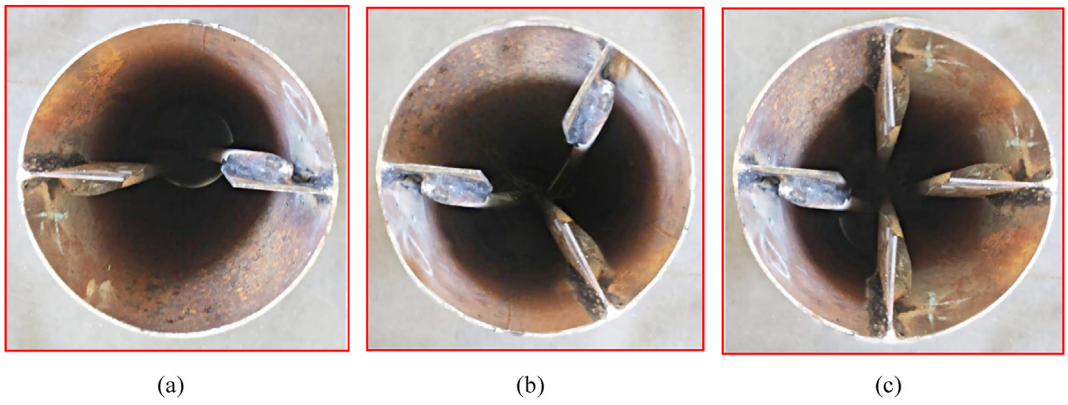

Fig. 2 – Catty-cornered propped CFST columns with various prop arrangements, (a) Binary Props, (b) Tertiary Props, (c) Quaternary Props.

NS means nano-silica, CNT means carbon nanotubes, NT means nano titanium dioxide. The specimens were prepared by inserting the catty-cornered props diagonally inside the steel casing and welding was to be provided to make the connection. After that concrete material was poured into the steel tube in three layers and compaction was done for each layer via vibrator. After that specimen was allowed to cure for 28 days with wet gunny bags. After curing the surrounding surface of the specimen was cleaned and the ends of the specimen were leveled with the help of a machine tool so that proper contact between the specimen ends and the loading machine can be achieved [43] (see Fig. 3).

2.2. *Material properties*

The mechanical properties of the steel casing were determined by performing tensile strength tests on the steel coupon specimen taken from steel tubes of diameter 180 mm and thickness of 3 mm. Similarly, tensile tests were accomplished to find out the material properties of prop bars of diameter 12 mm used as catty-cornered props. The strength value corresponding to 0.2% proof strain was employed as yield strain for the specimen. After accomplishing the tensile tests, the average yield strength of steel tube and prop bars were calculated as 320.5 N/mm^2 and 342 N/mm^2. Table 2 demonstrate the mechanical properties of steel tube and prop bar.

Further, the mechanical properties of normal concrete material were found out through cube compression tests. Cubical specimens were prepared of dimensions as 150 mm and a concrete mix of M30 grade was utilized to fill the moulds. The curing of cubes was done for 28 days and outcomes of compression tests showed the cube strength as 38.5 N/mm^2. Further the nano concrete was prepared by adding nano-silica, carbon nanotubes, and titanium dioxide in powder form to the normal concrete mix. The highest compression strength of concrete was observed for 2–3% nano-silica addition in concrete [44–49]. The efficiency of carbon nanotubes in general is

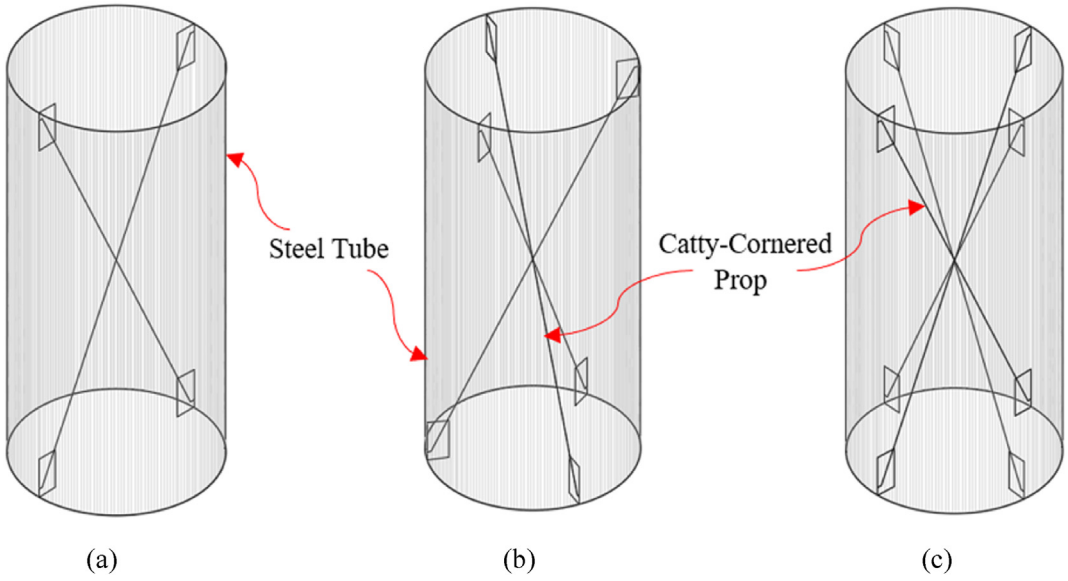

Fig. 3 – Catty-cornered propped CFST columns, (a) Binary Propped CFST, (b) Tertiary Propped CFST, (c) Quaternary Propped CFST.

Table 1 – Descriptions of column specimens.

Specimen	Diameter of Prop, d (mm)	No. of Props	f_{cu} (MPa)	f_{yp} (MPa)
UC	–	–	38.5	–
UC-NS	–	–	50.0	–
UC-CNT	–	–	44.0	–
UC-NT	–	–	42.0	–
BSC	12	2	38.5	342
BSC-NS	12	2	50.0	342
BSC-CNT	12	2	44.0	342
BSC-NT	12	2	42.0	342
TSC	12	3	38.5	342
TSC-NS	12	3	50.0	342
TSC-CNT	12	3	44.0	342
TSC-NT	12	3	42.0	342
QSC	12	4	38.5	342
QSC-NS	12	4	50.0	342
QSC-CNT	12	4	44.0	342
QSC-NT	12	4	42.0	342

US=Unstiffened CFST; BSC=Binary Stiffened CFST; TSC=Tertiary Stiffened CFST; QSC = Quaternary Stiffened CFST; NS=Nano-silica; CNT=Carbon Nano Tubes; NT=Nano Titanium Dioxide.

greater during initial ages and reduced with increasing the CNT percentage from 0.05 to 0.5% [50–53]. Also, the optimum dosage of NT lies in the range of 1–4% [54–56]. For the intended study, only initial percentages of nanomaterials were considered to modify the concrete. The proportions of nanomaterials used were 2% nano-silica, 0.05% carbon nanotube, and 1% nano titanium oxide. The properties of the nanomaterials utilized were presented in Table 3. The proportions of nanomaterials used to prepare concrete and properties of normal and nano concrete are presented in Table 4.

2.3. Test setup and measurement

To determine the uniaxial response of the suggested column section with nanomaterials-based concrete compression tests were accomplished at a loading rate of 0.5 mm/min employing the loading machine with the capacity of applying load up to 3000 kN on the specimen. The prepared specimens were tested after 28 days of curing of concrete. The specimens were set down in between the loading plates of the loading machine and the longitudinal axis of the specimen was made truly vertical so that no eccentric effect affect the results. Prior to commencing the compression, the top end of the specimen and loading plate were made in contact by applying a seating load of roughly equal to 10% of the estimated load capacity of the specimen. To record the observations of axial deformation, a dial gauge was provided at the mid-height of the specimen, and strain gauges were also employed to measure the strain values at the mid-height of the specimen. The experiments continued till the failure occurred in the specimen. The results of the strain gauge were collected from the data loggers and displacement results were noted from the dial gauges. The schematic arrangement of the experimental setup is presented in Fig. 4.

Table 2 – Mechanical properties of steel casing and catty-cornered prop.

Type	Yield strength (f_y), N/mm^2	Ultimate strength (f_u), N/mm^2	Elastic modulus (E_s), N/mm^2
Steel Tube	320.5	435.6	2.13×10^5
Catty-Cornered Prop	342.0	450.0	2.08×10^5

Table 3 – Physical properties of Nanomaterials.

Properties	Nano-silica (NS)	Carbon nanotube (CNT)	Nano Titanium dioxide (NT)
Particle size	10–20 nm	20–100 nm	50–200 nm
Specific surface area	200 m^2/gm	50–200 m^2/gm	60 m^2/gm
Unit weight	2.6 gm/cm^3	2.3 gm/cm^3	3.5 gm/cm^3
Colour	White	Black	White

2.4. Ductility index

The ductility index (DI), which has previously been used in many pieces of research, is used to evaluate the ductile performance of the stiffened CFST column [57,58]. The specimen's potential for inelastic deformation after the yield point can be expressed by the ductility index. The ductility index is represented as follows in Eq. (1) [57,58]:

$$DI = \frac{\Delta_u}{\Delta_y} \quad (1)$$

The symbol Δ_u stands for the specimen's ultimate displacement, which is calculated at the point where load capacity reaches 0.95 times its maximum value on the post-peak side. The yield displacement is symbolized by the symbol Δ_y, and it is computed as $\Delta_{0.75}/0.75$, where $\Delta_{0.75}$ indicates the deformation value corresponding to load capacity when it is reduced by 0.75 times the maximum capacity of the pre-yield side of the curve. The higher the ductility index, the slower the drop in load capacity after reaching maximum capacity [33].

3. Experimental results and discussion

The uniaxial compression performance of catty-cornered propped CFST columns was assessed by employing infill concrete properties enhanced with nanomaterials. The results for each specimen from the analysis were recorded for ultimate loading capacity, load vs deformation behavior, load vs strain behavior, ductility index and confinement effect, etc. The ultimate load capacity for all specimens is presented in Table 5.

3.1. Ultimate load capacity

The maximum axial load capacity of unstiffened, binary stiffened, tertiary stiffened, and quaternary stiffened specimens with a variation of infill concrete enhanced with nanoparticle additions was assessed and presented in Fig. 5. The

Table 4 – Properties of concrete.

Type	Nanomaterial and percentage of replacement	Cube compressive strength (f_{cu}), N/mm^2	Elastic modulus (E_c), N/mm^2
Normal Concrete	–	38.5	3.15×10^4
Concrete-NS	Nano silica, 2%	50	3.50×10^4
Concrete-CNT	Carbon nanotubes, 0.05%	44	3.35×10^4
Concrete-NT	Nano titanium dioxide, 1%	42	3.25×10^4

axial load capacity of the CFST specimen was upgraded by providing prop bars stiffening arrangement. Also, infill concrete with nanoparticle additions reflected a significant impact on the axial load capacity of unstiffened and stiffened CFST columns. It was observed as the stiffening arrangements were provided in the CFST specimen an increase of 12%, 16%, and 20.6% in the load-carrying capacity occurred in the case of binary, tertiary, and quaternary stiffening schemes respectively. Also, when 2% of nano-silica was incorporated in concrete infill, ultimate capacity upgraded by 10%, 14%, and 18% for binary, tertiary, and quaternary stiffened CFSTs as compared with the unstiffened specimens. However, when carbon nanotubes (0.05%) and nano titanium dioxide (1%) were added to concrete, improvement in ultimate capacity was recorded as 7%, 11%, 16%, and 8%, 12%, 15.4% respectively as compared with CFST specimens with normal concrete in case of binary, tertiary and quaternary props. The increase in load capacity was higher in the case of quaternary stiffened CFST with concrete infill properties enhanced with nano-silica. The addition of nanoparticles consequence in higher pozzolanic activities leading to more production of calcium-silicate-hydrated (C–S–H) gel due to its least specific surface area, as lesser the specific area more rapid is the hydration process resulting in better hydration products and also resulted in lesser porosity in concrete infill [9,14,59]. The addition of nanomaterials increased the strength of concrete infill which improved the ultimate capacity of CFST specimens. It was demonstrated by the findings of ultimate capacity that a relative increase in load capacity from unstiffened to binary stiffened to tertiary stiffened to quaternary stiffened CFST occurred at approximately 12%, 4%, and 5% respectively. Similar results were noted for CFST with nanomaterials-modified concrete. It indicated that the binary stiffening scheme led to a greater increase in the load capacity and further increased the number of props although resulted in more increase in the capacity of the column, however, relative to the binary props increase is not as high as for the binary case relative to unstiffened one. Among the nanomaterials, nano-silica showed a greater increase in the load capacity as can be observed in Fig. 5. For unstiffened

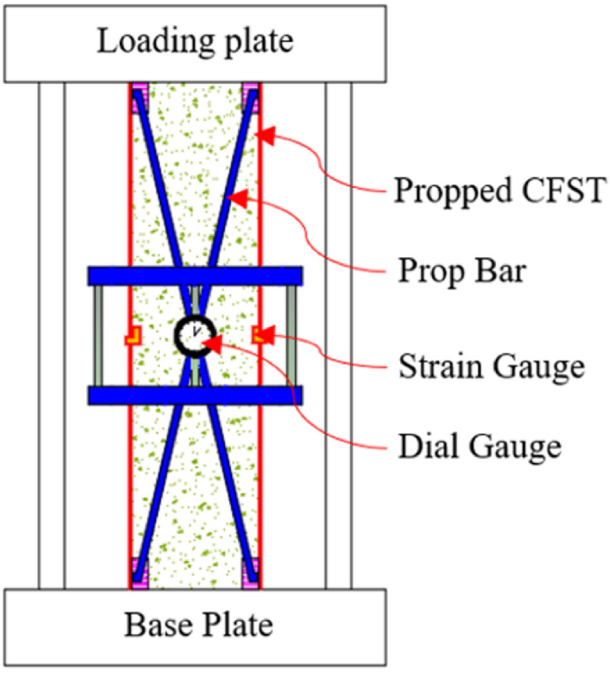

Fig. 4 – Schematic diagram for test arrangements of catty-cornered propped CFST specimen.

Table 5 – Ultimate capacity, ductility index, and secant stiffness of stiffened CFST with different infills.

Specimen	No. of Props	Axial load carrying capacity, P_u (kN)	Ductility index, DI	Secant stiffness, (kN/mm)
UC	–	1700	2.53	348.36
UC-NT	–	1775	2.48	355.00
UC-CNT	–	1856	2.44	360.39
UC-NS	–	1981	2.36	370.28
Average		1828	2.45	358.51
Standard Deviation		120.26	0.072	9.26
BSC	2	1901	2.93	358.68
BSC-NT	2	1952	2.88	364.86
BSC-CNT	2	1992	2.84	368.89
BSC-NS	2	2145	2.79	376.32
Average		1997.5	2.86	367.19
Standard Deviation		105.15	0.059	7.4
TSC	3	1975	3.42	369.16
TSC-NT	3	2017	3.36	375.61
TSC-CNT	3	2065	3.32	381.00
TSC-NS	3	2215	3.27	388.60
Average		2068	3.34	378.59
Standard Deviation		104.67	0.063	8.24
QSC	4	2050	3.89	377.53
QSC-NT	4	2095	3.84	382.30
QSC-CNT	4	2150	3.78	386.00
QSC-NS	4	2285	3.73	393.97
Average		2145	3.81	384.95
Standard Deviation		101.9	0.07	6.94

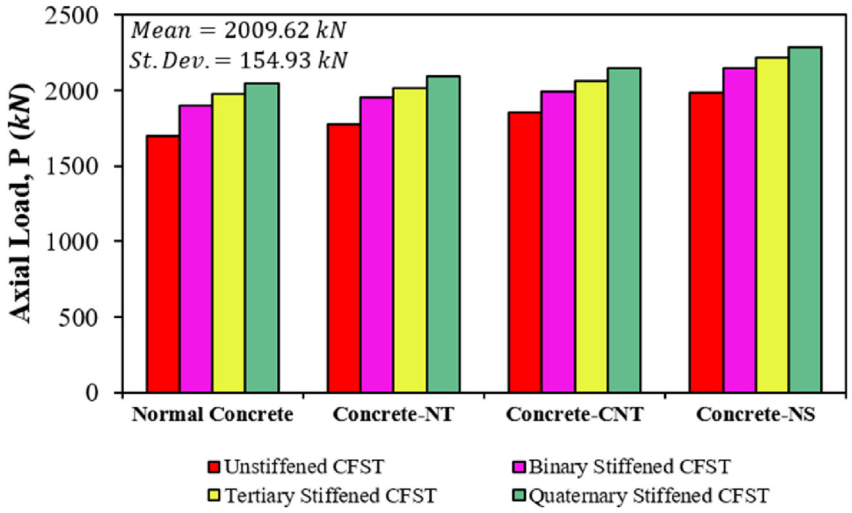

Fig. 5 – Maximum axial load capacity for stiffened CFST infilled with different concrete.

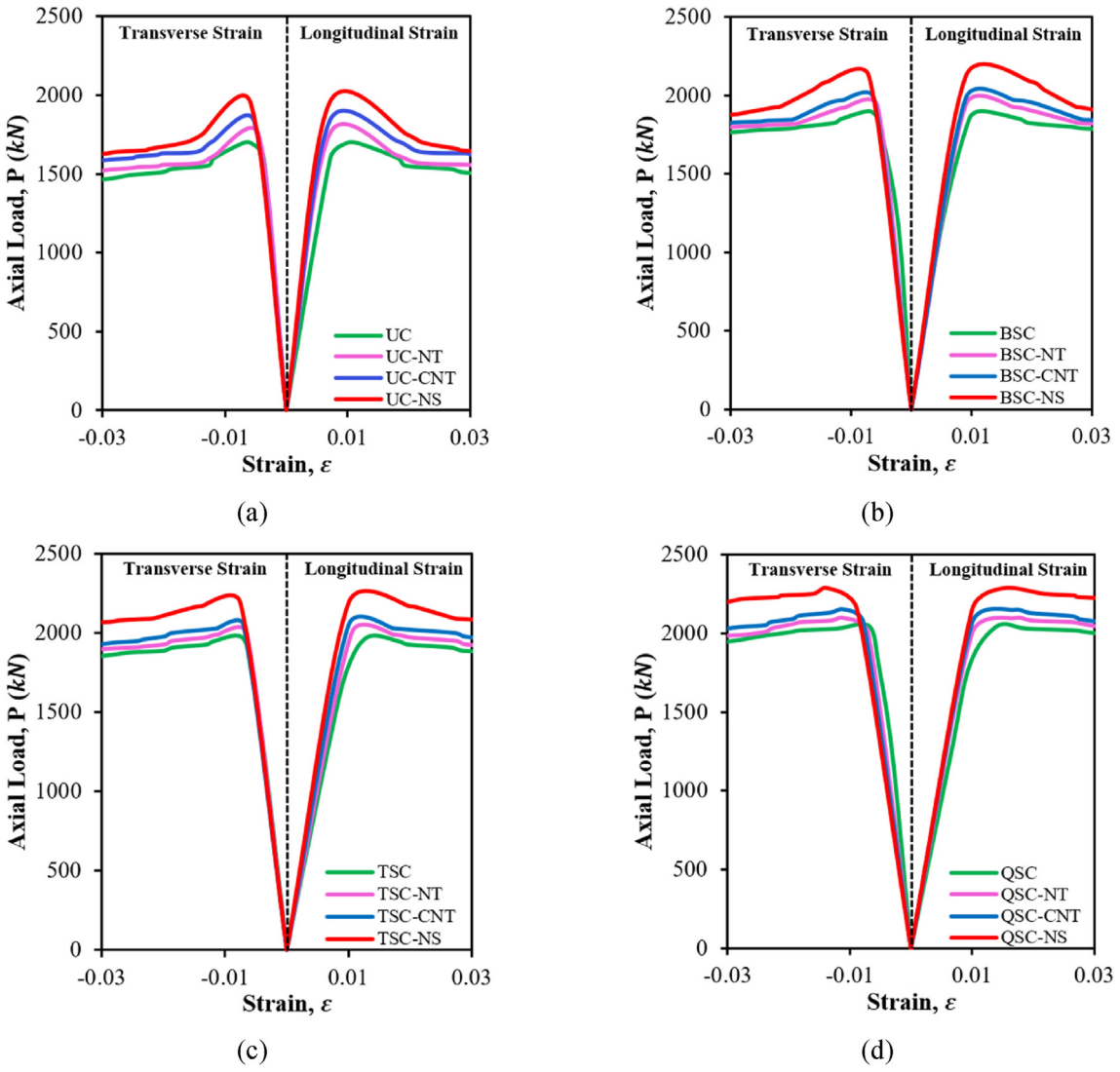

Fig. 6 – Load-strain curves for catty-cornered propped CFST with different infills, (a) Unstiffened specimens, (b) Binary stiffened specimens, (c) Tertiary stiffened specimens, (d) Quaternary stiffened specimens.

specimens, 16.5%, 9.2%, and 4.4% increase in load capacity was recorded in the case of nano-silica, carbon nanotubes, and nano titanium dioxide modified concrete infill steel tube columns respectively. Similarly, a greater increase in load capacity in the case of CFST with nano-silica-modified concrete was observed for binary, tertiary, and quaternary stiffened CFSTs.

3.2. *Load vs strain response*

The axial load vs transverse and axial strain response was recorded for stiffened CFST with concrete strength modified with nanomaterials. The load vs strain curves are depicted in Fig. 6(a–d). As indicated by Fig. 6 pre-peak and post-peak behavior of tested specimens improved with the addition of nanomaterials and increasing the number of catty-cornered bars. It was noted that during the initial phases of loading transverse strain development was slower as compared with axial strain for all the specimens. Further, in the case of CFST specimens with normal concrete transverse strain development was at a slower rate as compared with specimens with nanomaterial-based concrete infill. It was also indicated from the load vs axial strain response that the pre-peak behavior of the specimen upgraded in the case of the specimen with nano-silica-based concrete infill as compared with other nanomaterial additions. The initial stiffness was observed to be improved in the case of nano-silica-based concrete-filled steel tube sections, followed by specimens with CNT-based concrete and NT-based concrete infill. Further, nanomaterial addition in the concrete infill of CFST increased the load carrying capacity but showed a higher decline in load vs strain curve after achieving peak capacity as compared with CFST specimen with normal concrete [60]. Similar behavior was observed for stiffened CFST section. However, the decline in the load vs strain curve was more for unstiffened specimens as compared with stiffened specimens. Moreover, the inclusion of a quaternary stiffening scheme in combination with nanomaterial-based concrete enhanced the post-peak response of the CFST specimen as indicated in Fig. 6 (d).

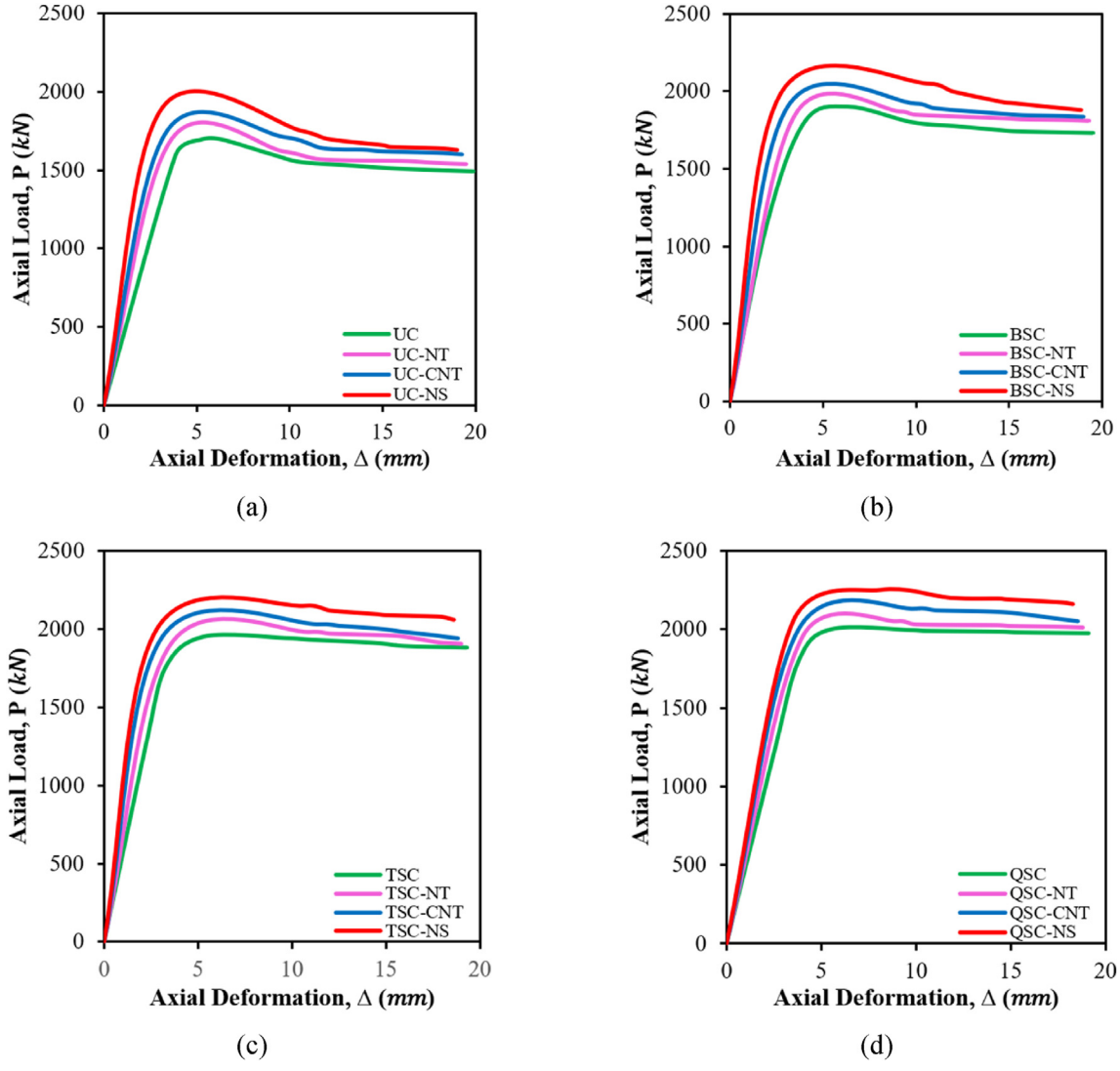

Fig. 7 – Load vs deformation curves for stiffened CFST with different infills, (a) Unstiffened specimens, (b) Binary stiffened specimens, (c) Tertiary stiffened specimens, (d) Quaternary stiffened specimens.

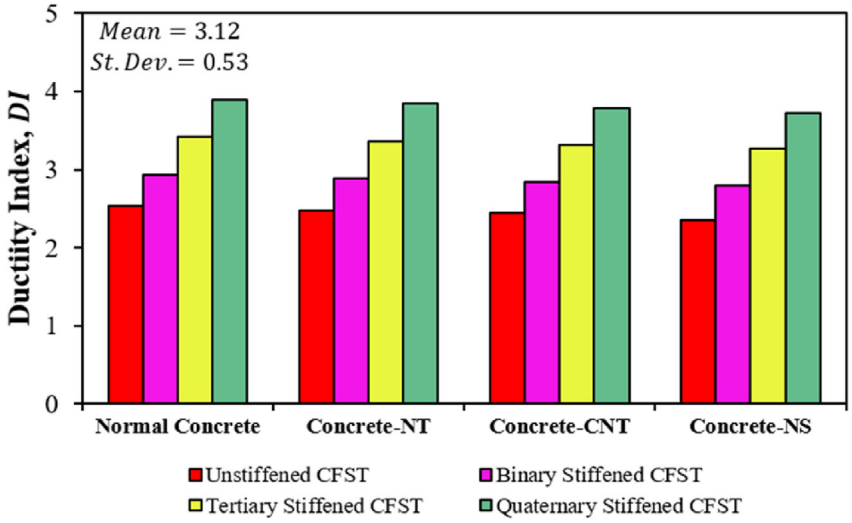

Fig. 8 – Ductility index for stiffened CFST infilled with different concrete.

3.3. *Load vs deformation response*

Fig. 7 depicts the axial load vs axial deformation behavior of stiffened CFST with nanomaterial-based concrete infill material. As discussed in the previous section that nanomaterial additions to concrete infill with stiffening arrangements in CFST enhanced the pre-peak and post-peak behavior of the column's specimen. The CFST specimens achieved maximum capacity at higher axial deformation when nanomaterial-based concrete was utilized as concrete infill in CFST specimens. Also, stiffening arrangements resulted in a reduction in axial deformation of CFST specimens, leading to higher stiffness. The ultimate capacity was achieved at approximately 4.88 mm, 5.3 mm, 5.35 mm, and 5.43 mm deformation values in the case of unstiffened CFST, binary stiffened, tertiary stiffened, and quaternary stiffened CFST specimens respectively. Similarly, maximum load capacity occurred at 5.43 mm, 5.48 mm, 5.57 mm, and 5.8 mm axial deformation of the specimen when normal, nano-silica-based, carbon nanotube-based, and nano titanium dioxide-based concrete was employed as infill material in quaternary stiffened CFST specimen. It was observed that with an increase in the number of stiffening bars maximum load capacity was achieved at higher deformation and a decrease in load capacity occurred less as compared with unstiffened specimens. Also due to the addition of nanomaterial-based concrete infill in the CFST specimen, maximum capacity was achieved at higher deformation and the decline in load capacity increased as compared with normal concrete infill. It indicated that due to the increase in strength of infill concrete, its brittleness increased resulting in a drop in load capacity after peak load. However, an increase in stiffening bars resulted in a higher steel ratio which improved the ductile behavior of the CFST column [61].

3.4. *Ductility index*

The effects of nanomaterial-based concrete and the suggested stiffening scheme on the ductility index of stiffened CFST specimens were investigated, and the findings of the stiffened

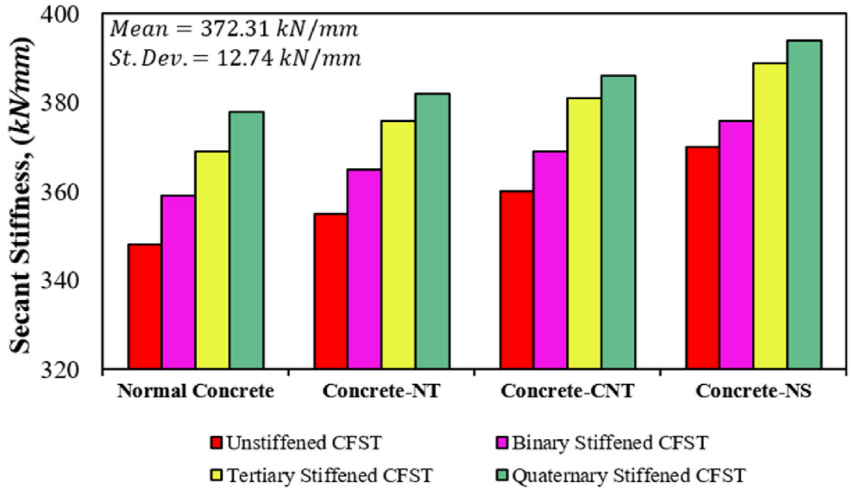

Fig. 9 – Secant stiffness for stiffened CFST infilled with different concrete.

CFST columns' ductility index with various concrete infills and stiffening scheme arrangements were shown in Fig. 8.

It was illustrated in Fig. 8 that the addition of the stiffening scheme and increasing the number of stiffening bars led to an improvement in the ductility index of the column section. However, CFST specimens with nanomaterial-based concrete infill showed a reduction in the ductility index of the specimen. The CFST columns with nanomaterials-modified concrete infill showed a higher drop in load capacity after peak load capacity as observed in load-strain and load–deformation behavior in previous sections. A greater drop in load capacity after peak load capacity indicates a reduction in ductility of the column section as the ductility index is the ratio of displacement corresponding to 95% of the peak load capacity on the post-peak side to displacement corresponding to the yield point [60]. It was due to an increase in the brittleness and stiffness of concrete infill due to the enhancement of concrete strength by nanomaterial incorporation in concrete, which showed cracking in the concrete post-peak reducing the capacity of the column at lower displacement [22,62]. It was recorded that nano silica-based concrete infill resulted in a higher decrease in the ductility index followed by carbon nanotube-based concrete infill and nano titanium dioxide-based concrete infill. The ductility index for all specimens tested is presented in Table 5. The reduction in ductility index was observed as 1.7%, 3.1%, and 5% as the normal concrete infill in the CFST column was replaced by concrete-NT, Concrete-CNT, and concrete-NS respectively. However, an increase in ductility index was recorded as approximately 17%, 36%, and 55% when binary, tertiary, and quaternary stiffeners were provided in CFST specimens.

3.5. *Secant stiffness*

The ratio of the column's ultimate load capacity to its displacement at that load is known as the secant stiffness [63]. The secant stiffness results for all specimens are presented in Table 5. The influence of different concrete infill and stiffening schemes on the secant stiffness of catty-cornered propped CFST specimens are depicted in Fig. 9 also. It was demonstrated that the proposed stiffening scheme reflected the improvement in the secant stiffness of the column section.

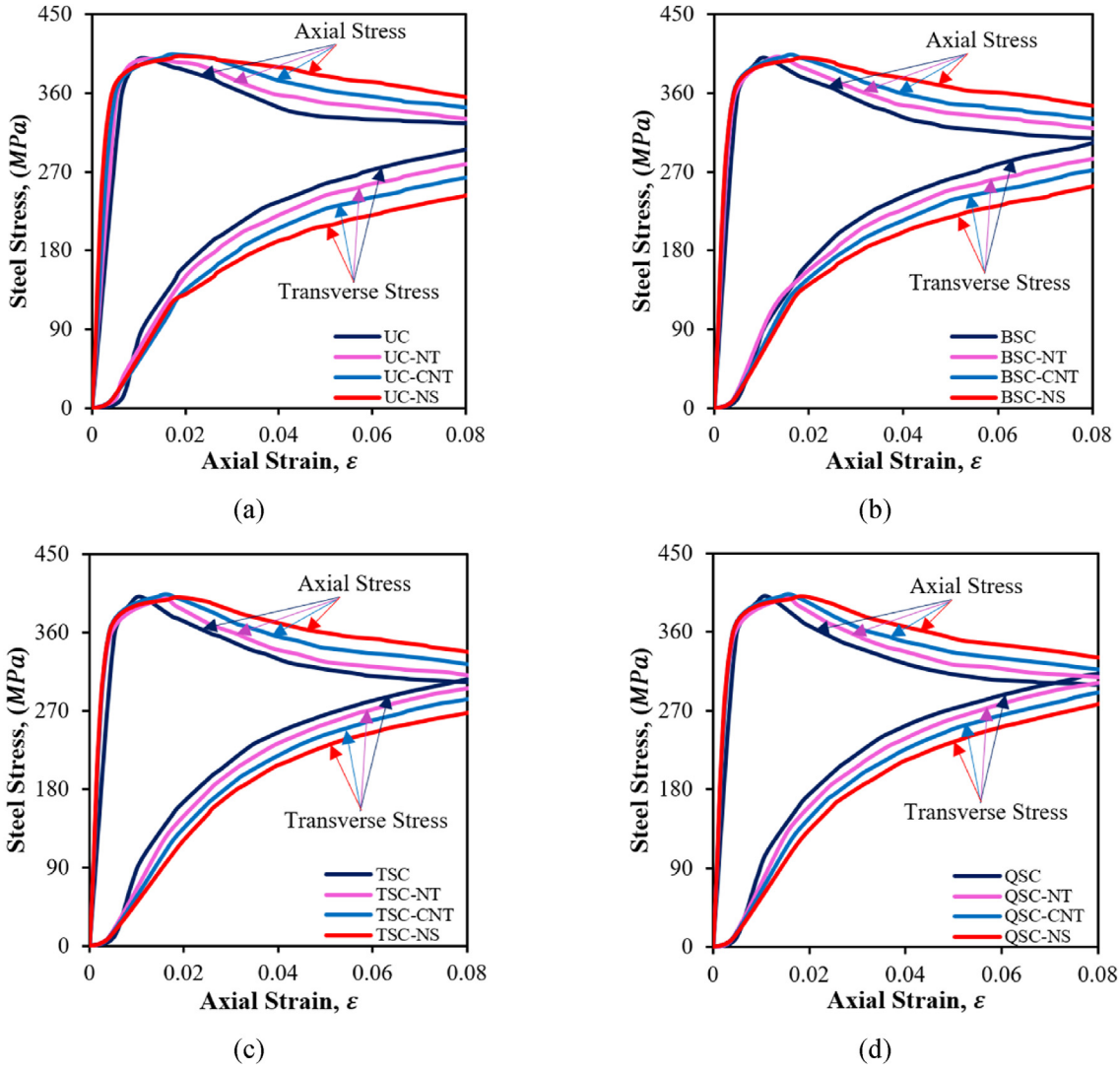

Fig. 10 – Steel stress variations for catty-cornered propped CFST with different infills, (a) Unstiffened specimens, (b) Binary stiffened specimens, (c) Tertiary stiffened specimens, (d) Quaternary stiffened specimens.

Further, enhancement of concrete strength by nanomaterial addition resulted in significant improvement of secant stiffness response of stiffened CFST. An increase of 1.65%, 2.9%, and 5.2% in secant stiffness values was recorded for unstiffened CFST sections when normal concrete was replaced by concrete-NT, concrete-CNT, and concrete-NS respectively. Further, an increase of 2.5%, 5.75%, and 7.5% was reflected in the case of binary stiffened, tertiary stiffened, and quaternary stiffened CFST specimens respectively as compared with unstiffened CFST. An increase in the concrete strength due to nanomaterials addition in the concrete infill of CFST resulted in a higher load to cause the deformation of the column specimen resulting in higher secant stiffness [13,16,64]. Further, as the stiffening bars increased load carrying capacity increased which leads to an increase in the stiffness of the section also.

3.6. *Steel stress variation*

The axial stress and transverse stress variation with respect to axial strain for the steel tube were evaluated to determine the influence of stiffening arrangements and infill concrete type on the confinement effect. The steel stress vs strain curves is presented in Fig. 10(a–d) for all the specimens. It was recorded that an increase in the number of stiffening bars resulted in a higher rate of development of transverse stress. As the transverse stress in the steel tube increased axial stress also decreased at the same time. At some point both the axial stress and transverse stress curves intersect. Earlier the intersection indicates that higher confining pressure on the infill concrete by the steel tube [33,65]. The longitudinal and transverse steel stress versus strain curves illustrates the composite interaction between the steel casing and the infill concrete [66]. As an increase in the number of stiffening bars resulted in an earlier intersection of axial and transverse stress, quaternary stiffened specimens were proved to have a higher confining effect on infill concrete. However, the enhancement of concrete strength by incorporating nanomaterials showed a decrease in the rate of development of transverse stress or reduction of axial stress of steel tube, leading to the later intersection of axial and transverse stress curves. The nano titanium-based concrete infill resulted in the

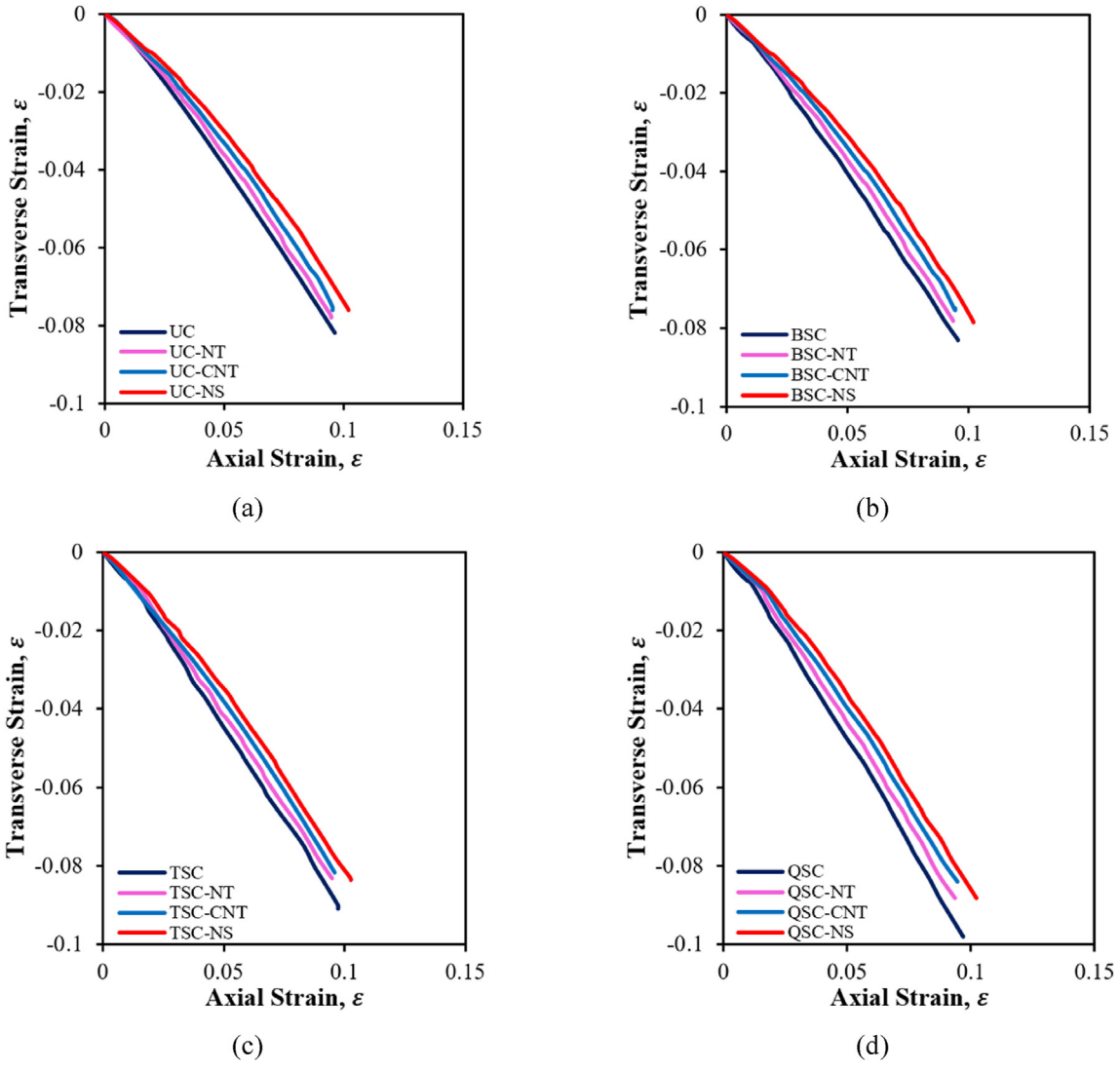

Fig. 11 – Lateral dilation response for catty-cornered propped CFST with different infills, (a) Unstiffened specimens, (b) Binary stiffened specimens, (c) Tertiary stiffened specimens, (d) Quaternary stiffened specimens.

decrease of confinement effect of unstiffened and stiffened CFST columns with normal concrete infill. Similarly, concrete-CNT, and concrete-NS further reduced the confining pressure. Due to addition of nanomaterials in concrete infill strength of concrete increased which caused reduction in the lateral expansion of concrete. The lateral forces exerted by concrete infill on the steel tube decreased resulting in lesser development of transverse stress in steel tube. It was concluded that quaternary stiffened specimens with normal concrete resulted in better confinement than other specimens.

3.7. *Lateral dilation behavior*

Fig. 11(a–d) shows the results of monitoring the lateral dilation response of stiffened CFST columns with respect to various stiffening arrangements and types of concrete infill. When the column specimen was loaded, the infill concrete began to expand and put pressure on the external steel casing. The stiffening bars enhanced the restraint on the infill concrete by steel casing and raised the perimetric strain in the steel tube. The higher the perimetric strain in the steel tube, the greater the confining force on the infill concrete [66]. The transverse strain development was more rapid in stiffened CFST columns as compared with unstiffened sections. It indicated that the addition of stiffening bars increased the constraining effect of steel tubes in the concrete infill [33]. Also, as the stiffening arrangements changed from binary to tertiary and quaternary schemes, an increase in confining forces was observed. However, specimens with concrete infill modified with nanomaterials additions resulted in a decrease in the development of lateral strain in steel tubes. The lateral strain development in steel tube decreased as normal infill concrete was replaced by concrete-NT, followed by concrete-CNT, and concrete-NS. It indicated that nanomaterial-based concrete decreased the composite interaction between steel tubes and infill concrete.

4. Conclusion

In this study, an experimental investigation was carried out to evaluate the axial load-bearing capacity and performance of the suggested catty-cornered propped CFST column section with concrete infill modified with nanomaterials compressed under concentric loading. The findings of the experimental study were evaluated in terms of ultimate capacity, load vs strain curves, and load vs deformation behavior. Further, the ductile behavior and stiffness variation w.r.t. Arrangements of stiffening bars and type of concrete infill were examined. The composite interaction and confinement effect of the proposed specimen were analyzed via steel tube stress variation and lateral dilation behavior. The uniaxial ultimate bearing capacity of the suggested stiffened CFST columns was greater than that of the unstiffened CFST columns. It was concluded that binary stiffening arrangement and nano-silica-based concrete were more effective and efficient in increasing the ultimate capacity of CFST specimens. The pre-peak behavior can be enhanced with the utilization of the suggested stiffening scheme and employing nanomaterials modified concrete. On the contrary post-peak response is improved through the stiffening scheme and a higher decline in load capacity was observed after achieving the ultimate capacity in the case of nanomaterials-based CFST. The quaternary stiffening scheme and concrete-NS were more effective in increasing the initial stiffness of CFST specimens. The ductile behavior of stiffened CFST columns improved with an increase in the number of stiffening bars. However, the ductility index was recorded to be decreased in the case of specimens with nanomaterial-based concrete infills. The tested specimens with a quaternary stiffening scheme and with normal infill concrete showed a better ductile response than other specimens. On the other hand, the quaternary stiffened CFST with nano-silica-based concrete infill resulted in higher secant stiffness. The composite interaction and confinement effect of steel tube and infill concrete was analyzed and results indicated that quaternary stiffened CFST specimens had more confining pressure on concrete infill and improved the composite interaction. However, the usage of nanomaterials in the concrete infill of CFST showed a reduction in the confinement effect and degrade the composite interconnection. The CFST sections with nano-silica-based concrete infill resulted in poor confinement as compared with specimens with other kinds of nanomaterial-based concrete infill and decreased the composite interaction. The use of nanomaterials in concrete applications as infill material for stiffened CFST can increase the cost in terms of their production, however, at the same time it is advantageous in enhancing the performance of stiffened CFST column in terms of strength, stiffness, load-strain behavior. The use of nanomaterials to enhance the properties of concrete infill of stiffened CFST column showed improved performance and is found to be feasible to use in this application.

Declaration of Competing Interest

The authors declare that they have no known competing financial interests or personal relationships that could have appeared to influence the work reported in this paper.

REFERENCES

[1] IEA-perspectives for the clean energy transition: the critical role of buildings. 2019.
[2] Santamouris M, Feng J. Recent progress in daytime radiative cooling: is it the air conditioner of the future? Buildings Nov. 30, 2018;8(12). https://doi.org/10.3390/buildings8120168. MDPI AG.
[3] Santamouris M, Vasilakopoulou K. Present and future energy consumption of buildings: challenges and opportunities towards decarbonisation. e-Prime - Advances in Electrical Engineering, Electronics and Energy 2021;1(Jan). https://doi.org/10.1016/j.prime.2021.100002.
[4] Palla R, Karade SR, Mishra G, Sharma U, Singh LP. High strength sustainable concrete using silica nanoparticles. Construct Build Mater May 2017;138:285–95. https://doi.org/10.1016/j.conbuildmat.2017.01.129.
[5] Reddy LSI, Vijayalakshmi MM, Praveenkumar TR. Thermal conductivity and strength properties of nanosilica and GGBS incorporated concrete specimens. Silicon Jan. 2022;14(1):145–51. https://doi.org/10.1007/s12633-020-00813-7.

[6] Qureshi LA, Ali B, Ali A. Combined effects of supplementary cementitious materials (silica fume, GGBS, fly ash and rice husk ash) and steel fiber on the hardened properties of recycled aggregate concrete. Construct Build Mater Dec. 2020;263. https://doi.org/10.1016/j.conbuildmat.2020.120636.
[7] Ozturk M, Karaaslan M, Akgol O, Sevim UK. Mechanical and electromagnetic performance of cement based composites containing different replacement levels of ground granulated blast furnace slag, fly ash, silica fume and rice husk ash. Cement Concr Res 2020;136(Oct). https://doi.org/10.1016/j.cemconres.2020.106177.
[8] Jha P, Sachan AK, Singh RP. Investigation on the durability of concrete with partial replacement of cement by bagasse ash (BAH) and sand by stone dust (SDT). In: Materials today: proceedings. Elsevier Ltd; 2020. p. 237–43. https://doi.org/10.1016/j.matpr.2020.11.652.
[9] Karakouzian M, Farhangi V, Farani MR, Joshaghani A, Zadehmohamad M, Ahmadzadeh M. Mechanical characteristics of cement paste in the presence of carbon nanotubes and silica oxide nanoparticles: an experimental study. Materials Mar. 2021;14(6). https://doi.org/10.3390/ma14061347.
[10] Vishwakarma V, Ramachandran D. Green Concrete mix using solid waste and nanoparticles as alternatives – a review. In: Construction and building materials. vol. 162. Elsevier Ltd; Feb. 20, 2018. p. 96–103. https://doi.org/10.1016/j.conbuildmat.2017.11.174.
[11] Bisht H, Gupta A, Srinivas D, Adak D. Structural performance of nano-silica based blended CFST stub circular column. In: IOP conference series: materials science and engineering. IOP Publishing Ltd; Dec. 2020. https://doi.org/10.1088/1757-899X/989/1/012003.
[12] Garas G, Sayed AM, Bakhoum ESH. Application of nano waste particles in concrete for sustainable construction: a comparative study. Int J Sustain Eng 2021;14(6):2041–7. https://doi.org/10.1080/19397038.2021.1963004.
[13] Allujami HM, Abdulkareem M, Jassam TM, Al-Mansob RA, Ibrahim A, Ng JL, et al. Mechanical properties of concrete containing recycle concrete aggregates and multi-walled carbon nanotubes under static and dynamic stresses. Case Stud Constr Mater Dec. 2022;17:e01651. https://doi.org/10.1016/j.cscm.2022.e01651.
[14] Praveenkumar TR, Vijayalakshmi MM, Meddah MS. Strengths and durability performances of blended cement concrete with TiO2 nanoparticles and rice husk ash. Construct Build Mater Aug. 2019;217:343–51. https://doi.org/10.1016/j.conbuildmat.2019.05.045.
[15] Kancharla R, Maddumala VR, Prasanna TVN, Pullagura L, Mukiri RR, Prakash MV. Flexural behavior performance of reinforced concrete slabs mixed with nano- and microsilica. J Nanomater 2021;2021. https://doi.org/10.1155/2021/1754325.
[16] Kansal CM, Goyal R. Analysing mechanical properties of concrete with nano silica, silica fume and steel slag. In: Materials today: proceedings. Elsevier Ltd; 2021. p. 4520–5. https://doi.org/10.1016/j.matpr.2020.12.1032.
[17] Shanmugam NE, Lakshmi B. State of the art report on steel-concrete composite columns. J Constr Steel Res 2001;57(10):1041–80. https://doi.org/10.1016/S0143-974X(01)00021-9.
[18] Kitada T. Ultimate strength and ductility of state-of-the-art concrete-filled steel bridge piers in Japan. Eng Struct 1998;20(4–6):347–54. https://doi.org/10.1016/S0141-0296(97)00026-6.
[19] Roeder CW. Overview of hybrid systems United for seismic States and composite design in the United Stated. Eng Struct 1998;20(4–6):355–63. https://doi.org/10.1016/S0141-0296(97)00035-7.
[20] Bradford MA, Loh HY, Uy B. Slenderness limits for filled circular steel tubes. J Constr Steel Res 2002;58(2):243–52. https://doi.org/10.1016/S0143-974X(01)00043-8.
[21] Zeghiche J, Chaoui K. An experimental behaviour of concrete-filled steel tubular columns. J Constr Steel Res Jan. 2005;61(1):53–66. https://doi.org/10.1016/j.jcsr.2004.06.006.
[22] Hossain KMA, Chu K. Confinement of six different concretes in CFST columns having different shapes and slenderness. International Journal of Advanced Structural Engineering Jun. 2019;11(2):255–70. https://doi.org/10.1007/s40091-019-0228-2.
[23] Sandeep Kauthsa Sharma M, Umadevi S, Sai Sampath Y, Vasugi K, Sai Nitesh KJN, Swamy Nadh V, et al. Mechanical behavior of silica fume concrete filled with steel tubular composite column. Adv Mater Sci Eng 2021;2021. https://doi.org/10.1155/2021/3632991.
[24] Vasanthi P, Selvan SS. Influence of nano SiO2 on structural behavior of concrete in-filled steel tube columns. Silicon Dec. 2021;13(12):4305–13. https://doi.org/10.1007/s12633-020-00746-1.
[25] Abendeh RM, Salman D, al Louzi R. Experimental and numerical investigations of interfacial bond in self-compacting concrete-filled steel tubes made with waste steel slag aggregates. Developments in the Built Environment Sep. 2022;11. https://doi.org/10.1016/j.dibe.2022.100080.
[26] Cai J, He ZQ. Axial load behavior of square CFT stub column with binding bars. J Constr Steel Res May 2006;62(5):472–83. https://doi.org/10.1016/j.jcsr.2005.09.010.
[27] Cai J, Long Y-L. Axial load behavior of rectangular CFT stub columns with binding bars. Adv Struct Eng 2007;10(5). https://doi.org/10.1260/136943307782417663.
[28] Liu HL, Cai J. Research on behavior of rectangular CFST stub columns with binding bars under axial compression. In: Applied mechanics and materials; 2013. p. 790–7. https://doi.org/10.4028/www.scientific.net/AMM.351-352.790.
[29] Tao Z, Han LH, Wang DY. Strength and ductility of stiffened thin-walled hollow steel structural stub columns filled with concrete. Thin-Walled Struct 2008;46(10):1113–1128, Oct. https://doi.org/10.1016/j.tws.2008.01.007.
[30] Wang Y, Yang Y, Zhang S. Static behaviors of reinforcement-stiffened square concrete-filled steel tubular columns. Thin-Walled Struct Sep. 2012;58:18–31. https://doi.org/10.1016/j.tws.2012.04.015.
[31] Yang Y, Zhang J, Wang Y. Experimental research on static behavior of stiffened square concrete-filled steel tubular columns subjected to axial load. In: Applied mechanics and materials; 2013. p. 1049–57. https://doi.org/10.4028/www.scientific.net/AMM.275-277.1049.
[32] Yang Y, Wang Y, Fu F. Effect of reinforcement stiffeners on square concrete-filled steel tubular columns subjected to axial compressive load. Thin-Walled Struct 2014;82:132–44. https://doi.org/10.1016/j.tws.2014.04.009.
[33] Ding FX, Lu DR, Bai Y, Zhou QS, Ni M, Yu ZW, et al. Comparative study of square stirrup-confined concrete-filled steel tubular stub columns under axial loading. Thin-Walled Struct Jan. 2016;98:443–53. https://doi.org/10.1016/j.tws.2015.10.018.
[34] Tao Z, Han LH, bin Wang Z. Experimental behaviour of stiffened concrete-filled thin-walled hollow steel structural (HSS) stub columns. J Constr Steel Res Jul. 2005;61(7):962–83. https://doi.org/10.1016/j.jcsr.2004.12.003.
[35] Zhang J, Liu Y, Yang J, Xu K. Experimental research and finite element analysis of concrete-filled steel box columns with longitudinal stiffeners. In: Advanced materials research; 2011. p. 1037–42. https://doi.org/10.4028/www.scientific.net/AMR.287-290.1037.
[36] Ling Y, Feng WY, Zhao JH, Li Y. Study on the ultimate bearing capacity of concrete filled steel square tubular short column with PBL. In: Advanced materials research. Trans Tech Publications Ltd; 2014. p. 770–5. https://doi.org/10.4028/www.scientific.net/AMR.941-944.770.

[37] Xu B, Wu F, Xu G. Mechanism study on the axial compressive performance of short square CFST columns with different stiffeners. Adv Civ Eng 2018;2018. https://doi.org/10.1155/2018/9109371.
[38] Liang W, Dong JF, Yuan SC, Wang QY. Behavior of self-compacting concrete-filled steel tube columns with inclined stiffener ribs under axial compression. Strength Mater Jan. 2017;49(1):125–32. https://doi.org/10.1007/s11223-017-9850-z.
[39] Huang CS, Yeh YK, Liu GY, Hu HT, Tsai KC, Weng YT, et al. Axial load behavior of stiffened concrete-filled steel columns. J Struct Eng 2002;128(9):91222. https://doi.org/10.1061/ASCE0733-94452002128.
[40] Hu H-T, Asce M, Huang C-S, Wu M-H, Wu Y-M. Nonlinear analysis of axially loaded concrete-filled tube columns with confinement effect. J Struct Eng 2003;129(10). https://doi.org/10.1061/ASCE0733-94452003129:101322.
[41] Wang H, Xu X, Zhou L, Zhang H, Yang F. The experimental study on concrete-filled thin-walled square steel tube short columns fixed U-shaped steel bars. In: Applied mechanics and materials; 2011. p. 962–9. https://doi.org/10.4028/www.scientific.net/AMM.94-96.962.
[42] Schneider SP, Member A. Axially loaded concrete-filled steel tubes. J Struct Eng 1998;124(10) [Online]. Available, https://ascelibrary.org/doi/abs/10.1061/. [Accessed 13 September 2022] (ASCE)0733-9445(1998)124:10(1125).
[43] Tiwary AK. Experimental investigation into mild steel circular concrete-filled double skin steel tube columns. J Constr Steel Res Nov. 2022;198. https://doi.org/10.1016/j.jcsr.2022.107527.
[44] Sun J, Shen X, Tan G, Tanner JE. Modification effects of nano-SiO2 on early compressive strength and hydration characteristics of high-volume fly ash concrete. J Mater Civ Eng Jun. 2019;31(6). https://doi.org/10.1061/(asce)mt.1943-5533.0002665.
[45] Behzadian R, Shahrajabian H. Experimental study of the effect of nano-silica on the mechanical properties of concrete/PET composites. KSCE J Civ Eng 2019;23(8):3660–3668, Aug. https://doi.org/10.1007/s12205-019-2440-9.
[46] Zhang MH, Islam J, Peethamparan S. Use of nano-silica to increase early strength and reduce setting time of concretes with high volumes of slag. Cem Concr Compos May 2012;34(5):650–62. https://doi.org/10.1016/j.cemconcomp.2012.02.005.
[47] Ghafari E, Costa H, Júlio E, Portugal A, Durães L. The effect of nanosilica addition on flowability, strength and transport properties of ultra high performance concrete. Mater Des 2014;59:1–9. https://doi.org/10.1016/j.matdes.2014.02.051.
[48] Kumar S, Kumar A, Kujur J. Influence of nanosilica on mechanical and durability properties of concrete. Proc Inst Civ Eng: Structures and Buildings Nov. 2019;172(11):781–8. https://doi.org/10.1680/jstbu.18.00080.
[49] Althoey F, Zaid O, Martínez-García R, Alsharari F, Ahmed M, Arbili MM. Impact of Nano-silica on the hydration, strength, durability, and microstructural properties of concrete: a state-of-the-art review. Case Stud Constr Mater Jul. 2023;18:e01997. https://doi.org/10.1016/j.cscm.2023.e01997.
[50] Cwirzen A, Habermehl-Cwirzen K, Penttala V. Surface decoration of carbon nanotubes and mechanical properties of cement/carbon nanotube composites. Adv Cement Res 2008;20(2):65–73. https://doi.org/10.1680/adcr.2008.20.2.65.
[51] Kim GM, Nam IW, Yang B, Yoon HN, Lee HK, Park S. Carbon nanotube (CNT) incorporated cementitious composites for functional construction materials: the state of the art. Composite structures, vol. 227. Elsevier Ltd, Nov. 01; 2019. https://doi.org/10.1016/j.compstruct.2019.111244.
[52] Hawreen A, Bogas JA, Kurda R. Mechanical characterization of concrete reinforced with different types of carbon nanotubes. Arabian J Sci Eng Oct. 2019;44(10):8361–76. https://doi.org/10.1007/s13369-019-04096-y.
[53] Abdalla JA, Thomas BS, Hawileh RA, Syed Ahmed Kabeer KI. Influence of nanomaterials on the workability and compressive strength of cement-based concrete. Mater Today Proc Jan. 2022;65:2073–6. https://doi.org/10.1016/j.matpr.2022.06.429.
[54] Meng T, Yu Y, Qian X, Zhan S, Qian K. Effect of nano-TiO 2 on the mechanical properties of cement mortar. Construct Build Mater Apr. 2012;29:241–5. https://doi.org/10.1016/j.conbuildmat.2011.10.047.
[55] Abdalla JA, Thomas BS, Hawileh RA, Yang J, Jindal BB, Ariyachandra E. Influence of nano-TiO2, nano-Fe2O3, nanoclay and nano-CaCO3 on the properties of cement/geopolymer concrete. In: Cleaner materials. 4. Elsevier Ltd; Jun. 01, 2022. https://doi.org/10.1016/j.clema.2022.100061.
[56] Siang Ng D, Paul SC, Anggraini V, Kong SY, Qureshi TS, Rodriguez CR, et al. Influence of SiO2, TiO2 and Fe2O3 nanoparticles on the properties of fly ash blended cement mortars. Construct Build Mater Oct. 2020;258. https://doi.org/10.1016/j.conbuildmat.2020.119627.
[57] Tao Z, Han LH, Zhao XL. Behaviour of concrete-filled double skin (CHS inner and CHS outer) steel tubular stub columns and beam-columns. J Constr Steel Res Aug. 2004;60(8):1129–58. https://doi.org/10.1016/j.jcsr.2003.11.008.
[58] Alqawzai S, Chen K, Shen L, Ding M, Yang B, Elchalakani M. Behavior of octagonal concrete-filled double-skin steel tube stub columns under axial compression. J Constr Steel Res Jul. 2020;170. https://doi.org/10.1016/j.jcsr.2020.106115.
[59] Li W, Ji W, Torabian Isfahani F, Wang Y, Li G, Liu Y, et al. Nano-silica sol-gel and carbon nanotube coupling effect on the performance of cement-based materials. Nanomaterials Jul 2017;7(7). https://doi.org/10.3390/nano7070185.
[60] Pagoulatou M, Sheehan T, Dai XH, Lam D. Finite element analysis on the capacity of circular concrete-filled double-skin steel tubular (CFDST) stub columns. Eng Struct Aug. 2014;72:102–12. https://doi.org/10.1016/j.engstruct.2014.04.039.
[61] Zhou X, Zhou Z, Gan D. Analysis and design of axially loaded square CFST columns with diagonal ribs. J Constr Steel Res Apr. 2020;167. https://doi.org/10.1016/j.jcsr.2019.105848.
[62] Manikandan KB, Umarani C. Understandings on the performance of concrete-filled steel tube with different kinds of concrete infill. Adv Civ Eng 2021;2021. https://doi.org/10.1155/2021/6645757.
[63] Tiwary AK, Gupta AK. Post-fire exposure behavior of circular concrete-filled steel tube column under axial loading. International Journal of Steel Structures Feb. 2021;21(1):52–65. https://doi.org/10.1007/s13296-020-00415-4.
[64] Ganesh P, Murthy AR, Kumar SS, Reheman MMS, Iyer NR. Effect of nanosilica on durability and mechanical properties of high-strength concrete. Mag Concr Res Mar. 2016;68(5):229–36. https://doi.org/10.1680/jmacr.14.00338.
[65] xing Ding F, Zhu J, Cheng SS, Liu X. Comparative study of stirrup-confined circular concrete-filled steel tubular stub columns under axial loading. Thin-Walled Struct Feb. 2018;123:294–304. https://doi.org/10.1016/j.tws.2017.11.033.
[66] xing Ding F, Luo L, Zhu J, Wang L, wu Yu Z. Mechanical behavior of stirrup-confined rectangular CFT stub columns under axial compression. Thin-Walled Struct Mar. 2018;124:136–50. https://doi.org/10.1016/j.tws.2017.12.007.